BIOENG-456: CONTROLLING BEHAVIOR IN ANIMALS AND ROBOTS

Mini Project:
Descending neurons control of leg kinematics and behavioral dynamics

Célia BENQUET, *Artur* JESSLEN *& Léa* SCHMIDT

Prof. *Pavan* RAMDYA

SPRING SEMESTER 2020

MAY 26, 2020

Contents

Abstract

In *Drosophila*, information from the brain to the nerve cord circuitry is conducted through only a few number of descending neurons (DNs). As a consequence, multiple behaviors with complex leg kinematics can be performed. This study aims at understanding how DNs drive such specific behaviors and if those behaviors can be clustered. To do so, we analyzed leg kinematics and behavioral dynamics in order to spot similarities between different strains of interest. By combining human curated and unsupervised clustering, it appears that multiple stereotyped behaviors can be driven from the activation of the same neuropils in the *Drosophila* ventral nerve cord. A deeper investigation of the MDN (Moonwalker Descending Neurons) and SS01540 (targeting DNp09) strains shows that they both drive transient behaviors. We hypothesized that those driven behaviors are used as fast behavioral defense mechanisms and that, as for MDN needing MAN (Moonwalking Ascending Neurons) co-activation for a persistent backward walking, DNp09 needs a co-activator to drive persistent fast forward walking. To confirm this hypothesis an experiment studying co-activation of DNp09 with other DNs or ANs could be done.

1 Introduction

As animals are evolving in a dynamic environment it is essential that their limb movements are well coordinated. Their survival depends on their ability to execute specific motor programs and to adjust motor output in response to external stimuli [1]. These mechanisms rely on the local motor circuits within the central nervous system, called central pattern generators (CPGs). In general, in insects, the motor circuits are located close to the muscles that they control in the ventral nerve cord (VNC), the insect motor control center, equivalent to the vertebrate spinal cord [1].

Proprioceptive feedback from leg mechanosensors ensure the accurate timing of each joint movement, but descending inputs acting on the CPGs are thought to be needed to adjust the order, timing or amplitude of individual leg movement [2]. These input signals are transmitted from the brain to the nerve cord through an estimate number of 250-550 pairs of descending neurons (DNs). Each of them synapses through a single axon onto interneurons associated with leg, neck and wing motor circuitry [3]. As the number of DNs is several orders of magnitude smaller than the number of neurons in both the brain and the VNC, this class of cells is a critical information processing bottleneck from sensory system to motor circuits [3], which may be problematic for information coding [1]. It is thus a strategic target for investigating the sensory-motor processing.

Several models have been proposed to explain how so few neurons can encode signals to control the full range of movement available to a freely moving fly. One hypothesis suggests that many stereotyped complex behaviors can be decomposed into individual motor modules controlled by the CPGs [1]. Such a proposition could not be investigated until recently. In 2014, Klapoetke et al. [4] discovered the channelrhodopsin Chrismon, used as on optogenetic tools to independently photo-activate a specific neuron population in a temporally precise fashion. Based on this new tool, Bidaye et al. [2] and Namiki et al. [3] designed respectively one and more than 100 transgenic strains of *Drosophila* expressing CsChrimson for the different specific DNs, allowing the community of the field to perform neurobehavioral studies. Hence, some recent studies suggest that driving a small subset of DNs could flexibly elicit multiple behaviors (Ijspeert et al. [5]). Reciprocally, multiple DNs could activate similar behaviors (Cande et al. [1]) and one behavior may result from the summed activity of DNs (Namiki et al. [3]). Finally, it was found that most of the DNs seem to trigger specific stereotyped behaviors such as walking or grooming. These behaviors can be represented in a 2D representation [1]. A deeper investigation of this last point will be our main focus in this project.

Those initial studies, while coming up with new lines of inquiry, provide limited details about how DNs control leg kinematics and behavioral dynamics. Therefore, 9 transgenic strains, the Moonwalker Descending Neuron (MDN) strain (Bidaye et al [2]) and 8 of the most interesting Namiki/Cande's strains were selected and new experiments were performed. From the resulting video data, more precise measurements were obtained for the body movement, using the 'Tracktor' computer vision software (Sridhar et al. [6]), and the leg joint positions, using the 'DeepLabCut' deep network-based pose estimation tool (Mathis et al. [7]).

With those data available, we first focus our study on 2 transgenic strains, the MDN and SS01540. The precise timing and characteristics of the resulting behavior are deeply described and discussed. Then, we analyze all the selected strains in order to find potential clusters in the set of DNs. The idea would be to gain insights on potential similar ways of action at the neural level and to better understand the role of DNs in the sensory-motor processing.

2 Methods

2.1 Experimental paradigm

The experiment takes place in arenas of 32 mm $\times$ 32 mm, where movements are limited to a 2D plane. The arenas are placed in a robotic high-throughput optogenetic system, *Optobot*, equipped

with a sCMOS camera that captures the flies behaviors from a ventral view and sees the limbs. The arenas, disposed on plates, are placed on a shelf and the robot puts the plates one by one under optogenetic illumination. Hence, we speak of light ON or OFF to precise if the arena is optogenetically illuminated or not at a given moment.

Nine transgenic *Drosophila* strains expressing CsChrimson in DNs were selected because their axon projects to the leg neuropils of the VNC and they drive leg-related behaviors. The data for those nine strains and for the PR negative control strain were obtained. For each strain, one arena contained three or two flies. Four replicas of the same experiment, were performed for each arena. One experiment goes as follow: 1.5 sec OFF, 3 sec ON, 10 sec OFF, 3 sec ON, 10 sec OFF, 3 sec ON, 1.5 sec OFF. All of the studied flies are females.

We analyze more thoroughly two of the tansgenic strains: the MDN strain, expressing CsChrimson in MDNs and the SS01540 strain, expressing CsChrimson in DNp09. We also analyze the PR negative control strain.

2.2 Data collection

Using *Tracktor* [6], it was possible to track the flies individually and to isolate them by mapping the movement of their center of gravity. This last one is used as the fly position to map the different kinematics and as one of the features for clustering to create the behavior maps. Then, *DeepLabCut* [7] was used to track the position of the head, abdomen, thorax, legs and wings, giving the 32 remaining features used for clustering.

2.3 Data analysis

The processing and plotting of the data are written using Python and presented on a Jupyter notebook.

The raw data are directly used to plot the position. For the other kinetics, a moving average filter (width = 30 frames = 0.375 s) is applied. It introduces some losses in the temporal precision but the results obtained are still better as it smooths the results and removes the noise. The velocity is computed by taking the difference of position of a fly between two frames. We can deduce the velocity from the frame rate (80 fps) and convert from px/s to mm/s (32 mm = 832 px). For the claws frequency, the instantaneous periods are computed as the time between two local peaks in the claws position. Then, the frequency is calculated using the inverse of the period. We also compute the average frequency over each experimental stage (ON and OFF) for each claw.

2.4 Clustering

To classify the different strains of interest into similar behaviors, we analyze the videos of each strain and interpret their main behavior on the ON periods. Subsequently, we observe the different strains innervation into flies VNC to find a consistency between the behavior and its corresponding neuron innervation. Those neurons projections are studied based on the Fly Light Split-Gal4 Driver Collection confocal image set [8].

2.5 Unsupervised clustering

To generate our clustering, we mainly follow the method presented by Barden et al. [9] and used in Cande et al. [1]. After the images from the arena are processed, their body centroid are identified. Their postural dynamics (high dimensional data) are projected on an euclidean space with less dimensions, using Principal Components Analysis (PCA). It is a dimensionality reduction technique that keeps dimensions that explain most of the data variance. Unlike in Barden et al., we use directly the position of the claws at each time frame (see Fig.5, Annexes), which are already low dimensional (12 dimensions by frame - x and y position for each leg). Thus, we do not have to use dimensionality reduction techniques.

To analyze the behaviors of the flies and their claw's dynamics, the wavelets transform (using Morlet's waves) is used on the claws' position. For each frame, by considering neighbors frames, we convert the positions of the different claws in wavelets. For that we use 25 frequency channels, dynamically spaced between 1 and 40 Hz, the Nyquist frequency of the system, to construct the spectrograms (spectral feature vectors). This process increases dimensionality. Therefore, those data are reduced using the t-distributed Stochastic Neighbor Embedding (t-SNE) (van der Maaten and Hinton [10]) and are embed into two dimensions, by keeping the notion of distances between points during the dimensionality reduction.

Then, for each strain a density graph is computed (Fig. 3) by applying a KDE (Kernel density estimation) on the data obtained from the 2D representation of leg kinematics in the reduced frame produced by the t-SNE (Fig. 2A). Similar behaviors at the same position in the maps are grouped into clusters on Figure 2B.

3 Results

3.1 Behavioral data

From the generated graphs and the videos, we observe that the flies of a same Gal4-line produce identical behaviors, at each trial and for the whole 3-seconds simulation period in a trial. We spot irregularities for some replicas, but by reviewing the raw video data, most of them are justifiable by the position of the fly in the arena or its speed at the time of the triggering. For the two Gal4-strains we deeply study, MDN and SS010540, the behavioral response to the stimulation is observable mostly by looking at the velocity and claws frequency of the fly through the experiment and the results presented on Figure 1.

Kinematic results for the negative control PR strain are presented on Figures 4 and 6 (Annexes). The velocity, trajectory in the arena and claws frequency are shown. The angular velocity was calculated for the 3 strains in the Jupyter notebook. Overall, PR flies do not show specific behaviors under optogenetic light stimulation.

Flies from the MDN strain walk backward upon optogenetic illumination and goes back to forward walking as soon as the stimulation ends. The kinematic analysis shows that the velocity goes down to negative values precisely when the light turns on (Fig.1B). Moreover, as seen on Figure 1C, the leg frequency along the y-axis decreases for all 6 legs. On the slow motion videos, a synchronisation seems to appear between the middle legs. Concerning their trajectories, they mainly stay on the border of the arena and return on their steps (Fig.1A).

SS01540 strain flies show a different behavior. When the stimulation turns ON, they speed up in the forward direction. From Figure 1E, there is a sudden transient peak of velocity at the beginning of the ON phase. Coherently, path length is extended and a larger area of the compartment is explored (Fig.1D). The frequency of the claws on the x-axis increases over the time of the stimulation (Fig.1F). Similarly to the MDN strain, the angular velocity stays low and close to what we observe for the control, which makes sense as they drive translational movement and not rotational movement.

For both strains, we could have expected a clearer plateau when the stimulation occurs but instead, once the initial transient burst has passed, the effect vanishes and the velocity for both strains gets closer to zero. When the light goes off, the flies are not constrained anymore and the DN-activated behaviors do not persist, letting them go back to a random wandering in the arena.

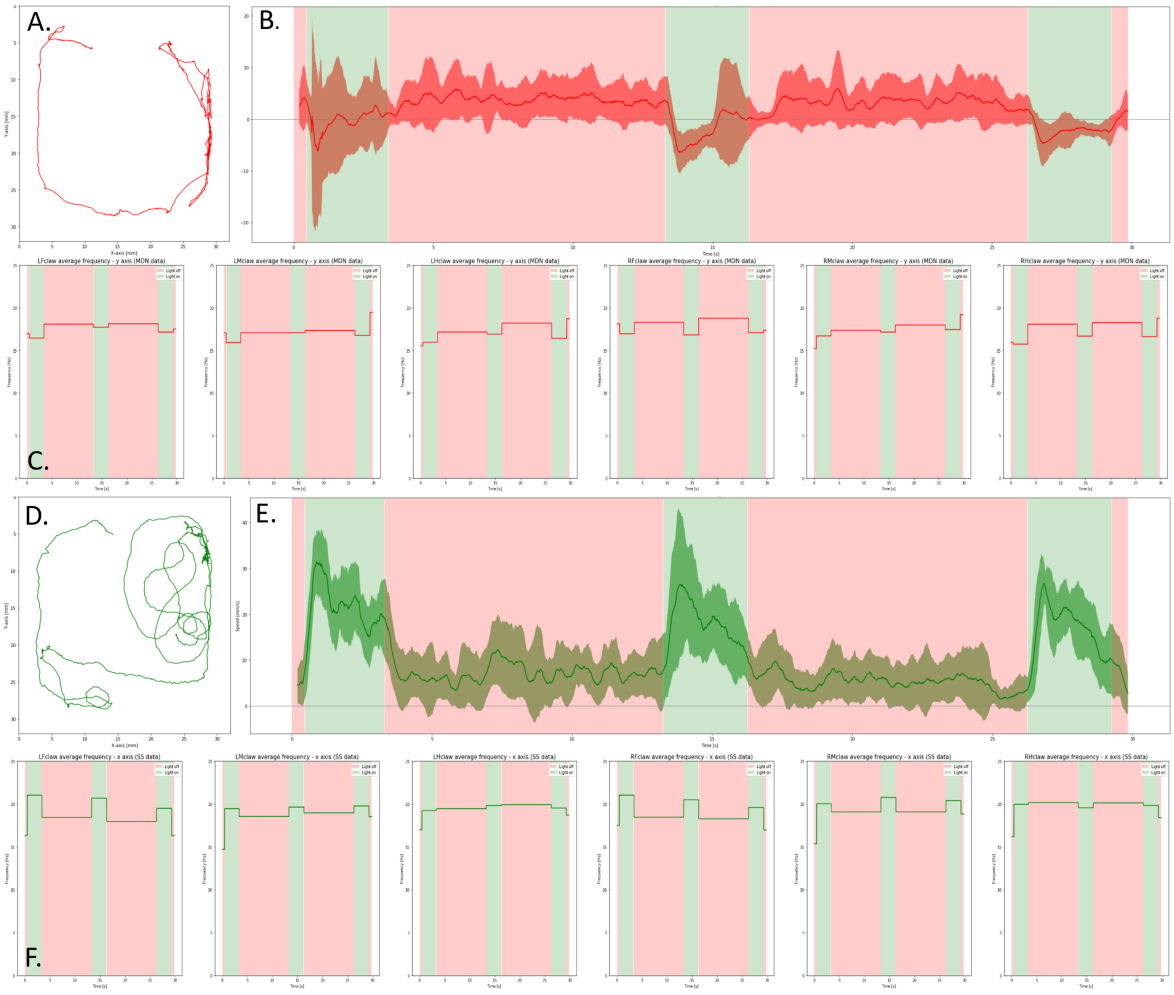

Figure 1: Kinematic results for MDN and SS01540 strains. (**A**-**C**) MDN strain. (**D**-**F**) SS01540 strain. (**A**, **D**) Position of the fly for one replica. (**B**, **E**) Averaged velocity of the strain over all replicas. Green parts: ON periods, Red parts: OFF periods. A moving average of 30 frames was used. (**C**, **F**) L: left, R: right, F: fore leg, M: middle leg, H: hind leg. A moving average of 30 frames was used. (**C**) Average frequency of the claws on the y-axis of the strain over all replicas. (**F**) Average frequency of the claws on the y-axis of the strain over all replicas. Results for the PR strains are presented in the Appendix.

3.2 Clustering based on videos and confocal images

On the videos, we observe a set of behaviors, specific to each of the 9 selected transgenic *Drosophila* strains. Even though some flies present more than one behavior during the stimulation, we focus on the main visible one. A detailed inspection shows that those specific behaviors present some similarities stated in Table 1. This table also depicts the different DNs neuropils innervation we observed on the corresponding confocal images. Except from the neck and wing innervations (which are complex to distinguish from a horizontal view), our observations are similar to the ones from Namiki et al [3].

Comparing the findings on Table 1, we observe different characteristic behaviors for strains with similar innervated neuropils. However, even if the behaviors per se are different, the part of the body

	Strains	Characteristic behaviors	Innervated neuropils
Forward walking	SS02279	More disjointed movements	bT1, bT2
	SS01540	High velocity at start, then decreases	bTect
Backward walking	SS02377	Only at start, followed by forward walking	bT1, bT2, ulT3
	MDN	Until end of stimulation	bT3, bAS
Grooming	SS02608	Anterior legs, right on stimulation	uT1
	SS01054	Posterior legs, beyond stimulation	bAS
Freezing	SS01049	Slow or still, beyond stimulation	bT1, bT2, bT3
Turning	SS02111	Change direction by turning, only once	bT1
	SS02617	Spinning on itself during the all stimulation	bTect

Table 1: Clustering of the selected transgenic strains based on visual observations. The characteristic behaviors were determined based on human curation of the raw videos. The innervated neuropils were determined thanks to confocal image analysis. T1: Prothoracic leg, T2: Mesothoracic leg, T3: Metathoracic leg, AS: Abdominal segment, Tect: Tectulum (b: bilateral, u: unilateral, l: left, r: right).

used to perform them are similar. For example, legs (T1, T2, T3) are targeted in both SS01049 and SS02377, driving reciprocally freezing, where the legs may be inhibited to prevent the fly from moving, and backward walking, where the legs should be activated to perform locomotion. Hence, both strains act on legs movement but in different ways.

3.3 Unsupervised Clustering

Results of the unsupervised clustering, based on leg kinematics of the flies, are shown on Figure 2A and 3.

For each strain, different peaks of density appear on the maps from Figure 3, which represent different behaviors. To realise the synthetic organization of our clustering (Fig. 2B) we kept the denser one. However, having those less obvious peripheral behaviors, more or less close to the main one, corroborates our visual observations. Indeed, it means that there are one main behavior as well as less visible ones happening for each strains during a stimulation.

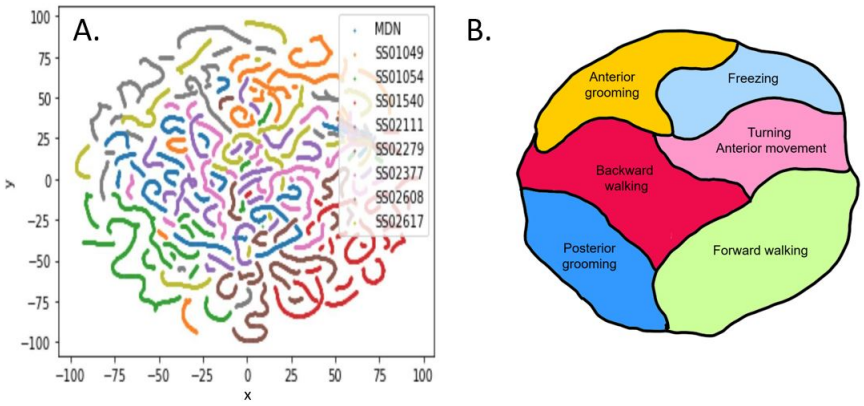

Figure 2: (**A**) 2D representation of leg kinematics in the reduced frame produced by the t-SNE. (**B**) Synthetic organization of the DN behavior space corresponding to the unsupervised clustering, based on human curation of (A) and KDE (kernel density estimation) regions in the space presented in Fig. 3.

4 Discussion

4.1 MDN and SS01540 driven behaviors

The experiment consists in a broad screening where leg-related movements are observed. However, different behavioral patterns are to be expected. The complexity lies in delimiting which behaviors are triggered by optogenetic illumination and which come from a "natural" behavior. A way to do so is to introduce a negative control strain. The PR strain doesn't express the Gal4-protein that binds to the UAS-CsChrimson and so, do not present optogenetic activation. By calculating the kinetic results for the PR strain, we obtain negative controls. We can compare them to the kinetics for the transgenic strains to analyze the behavioral changes driven by optogenetic stimulation.

The two transgenic strains drive different behaviors: accelerating and moving backward. We will first discuss results for the MDN strain, as it was extensively studied by Bidaye et al.[2], then generalize to the SS01540 strain, targeting DNp09. The transient burst in velocity that we observed in section 3.1 could be generated by an activation of the driven behavior without inhibiting the opposite behavior (here, forward walking). Hence, other behaviors, taking the upper-hand on the driven one, could make the backward velocity progressively decrease. Moreover, backward walking ends as soon as the stimulation ends. Those two points corroborate Bidaye's findings that MDN neurons activate backward walking but for the behavior to be persistent it requires the co-activation of ascending neurons MAN [2]. We hypothesize that the DNs bottleneck effect ([1],[3]) results in a hierarchical selection of the behavior to effectuate. In natural conditions, MDNs are activated either by antennae contact (obstacle avoidance) or when sensing a danger ahead [2]. They are important to convert threatening visual

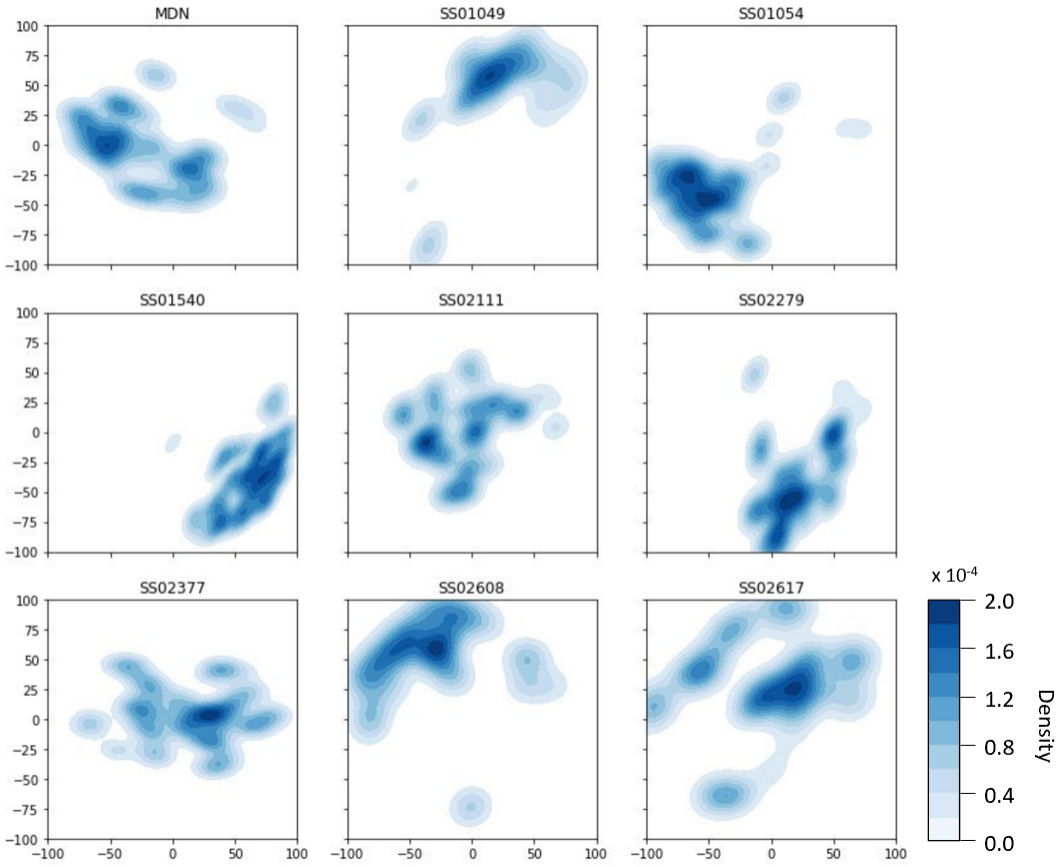

Figure 3: Behavioral probability density maps for all the studied strains. The region graphs are computed by applying a KDE (Kernel density estimation) on the data for each strain obtained from the 2D representation of the leg kinematics in the reduced frame produced by the t-SNE (Fig. 2A) for each strain.

stimuli into directional locomotive output [11]. Concerning SS01540, DNp09 may be used to flee from danger faster and so would be useful for survival. We hypothesize that the flies need those fast and transient behaviors as defense mechanisms to quickly escape (either by changing direction or running away) before flying away. By extension, because they show similar variations in kinetics and they supposedly both drive defensive mechanisms, a persistent fast forward walking could require a similar co-activation while the DNp09 neurons only initiate the behavior.

4.2 Behavioral Clustering

Our observational classification of the strains based on similar behaviors can be related to the morphology of DNs axon terminals within the VNC, where higher order decisions are transformed into actions (as presented in the section 3.1). The VNC contains neuropils which control motor outputs for distinct parts of the body including the neck, the wings, the tectulum, the lower tectulum as well as the

anterior, middle and posterior legs [12]. It is divided into 2 lateral parts and the DNs can target one (unilateral) or both (bilateral) of them.

As said in the section 3.1, with the same neuropils innervation, different behaviors can be achieved. Hence, by looking at the morphology of DN axon terminals within the VNC, one can predict which body part is targeted but not with what effect (inhibitory or excitatory signal, driving basic or more complex coordination of movement such as grooming). Nevertheless, it can provide supplementary knowledge on how the behavior is driven, that an analysis of the video would not. For instance, for strain SS02279, we observe a forward walking behavior. By coupling it to the innervations of the DNs (bT1 and bT2), it is shown that instead of targeting all 6 legs, only the front and middle legs are activated, and so the back legs may just follow the movement. Similarly, if the innervation is unilateral, one side may drive the movement while the other one just follows (see SS02608 with both anterior legs grooming while the innervation is uT1) .

In order to perform unsupervised clustering of DN optogenetically activated behaviors, we use a method introduced by Berman et al.[9], as explained in detailed in the section 2.5. Another approach, performed by DeAngelis et al. [13], consists in representing the data in low-dimensionality, using the nonlinear dimensionality reduction algorithm UMAP (McInnes et al. [14]). As for the precedent approach, the data are first converted in time series and normalized but UMAP does not process them the same way. It preserves the local and global topology of the high-dimensional data, whereas t-SNE emphasizes local structure at the expense of global structure [13]. Nevertheless, this last method was not implemented because of its complexity and the fact that we had many behaviors to analyze. The 3D resultant representation would not allow the results analysis and clustering to be as representative and meaningful as the results we obtained using the t-SNE method and its 2D resultant representation.

Overall, the human curated and unsupervised clustering are alike. However, the behavioral map obtained using unsupervised clustering (Fig.2B) contains 6 actions, whereas we obtain 5 classes from our visual clustering. Indeed, we define anterior and posterior grooming as one group of similar behaviors when the algorithm does not classify them as similar movements and so does not put them close to each other in the cluster space. It makes sense as they activate opposite pairs of claws (on transverse plane)

Visually near behaviors are close in the behavioral map. For example, flies performing anterior grooming stay static, similarly to freezing. We observe that the two behaviors are indeed next to each other in the cluster space on Figure 2B. On another point, some flies present multiple behaviors on Figure 3. While the main emerging behavior corresponds to the one we report on Figure 2B, peripheral observed behaviors still appear close to it on the map. For instance, strain SS02377 drives

backward walking, quickly followed by forward walking while stimulation is still ON. Coincidentally on the corresponding behavioral map, we see a dense area in the backward walking cluster as well as a light area in the forward walking cluster. Hence, similar behaviors driven by different strains are clustered close together, which corroborates the idea that distance in cluster space relates well to visually perceived similarities. Reciprocally, different behavior driven by the same strain are clustered close together.

4.3 Strengths and limits of the experiment design

As the experiment aims at providing a detailed analysis of how DNs control more specifically leg kinematics and behavioral dynamics, it is designed to highlight those data. As they were studied in other papers (Cande et al. [1], Namiki et al. [3]), the selected DNs are known to drive obvious and leg-related behaviors. The experiment set-up might be designed to facilitate the driven behaviors by establishing a suitable context, as it was shown to be useful by Cande et al. [1]. The arenas are bigger than in the previous experiments of that kind, which promotes freer movements, even if the flies are still not in a near-natural environment. The flies can have social interactions, which is thought to facilitate grooming behaviors, especially in females [15]. The introduction of the social factor could also be a way to test the results of Cande et al. as the experiments are really similar and they already tested non-social behaviors for those strains. However, it allows a lot of other behaviors, unwanted in the experiment, such as collision, which is likely to happen in a restricted area with driven locomotion behaviors. If we were able to collect the data ourselves, we would have chosen to isolate the flies, as in Cande et al. [1] and, by so, restrain all kind of social behaviors. In both experiments, other kind of behaviors, such as sexual behaviors or flying, are restrained, which limits peripheral behaviors that would add noise to the analysis. A non-negligible factor of the set-up is the fact that the flies have to evolve in a closed restricted area. They could react differently than in a natural environment and the use of virtual reality could be a way to check that.

Concerning the data collection, due to the limits of the video resolution, behaviors occurring over time-scales faster than the Nyquist frequency of the system, 40 Hz, are not detectable. It is less precise than for Cande's experiment [1] (50Hz), but the need for such a high precision is questionable regarding the obvious behaviors we observe. Cande's set-up consists in 30 repetitions of ON and OFF periods of respectively 15 and 45 seconds. In comparison, the 3-seconds ON periods in our set-up may seem short and they get more data for each fly, for both ON and OFF periods. This implicates that their statistical analysis should be better than ours. However, they realized that most of the driven

behaviors are transient and diminish after a few seconds. As our selected strains present such a transient kinetic (section 3.1), it may explain why it was decided to have a short stimulation period in our experiment. Moreover, they get their data differently. While we use *Tracktor* and *DeepLabCut* to get detailed and precise features, they only isolate the body pixels and use them directly as features for the clustering. This should allow us to get a more precise clustering. However, we only select 9 strains to perform our behavioral map, which is not enough to assess a good precision and is significantly smaller than the 133 strains Cande et al. studied.

4.4 Further investigations

As hypothesized in the section 3.1, some behaviors might be more important and enforce themselves on others. We also know that for MDN to drive a persistent motion MAN needs to be co-activated. To know more about this potential hierarchy and co-working neurons, further studies are needed, for instance by investigate the SS01540 strain deeper. We could also think about activating 2 strains at the same time. It would show us if they are working together and if not which strains have the highest importance.

References

[1] Jessica Cande, Shigehiro Namiki, Jirui Qiu, Wyatt Korff, Gwyneth M. Card, Joshua W. Shaevitz, David L. Stern, and Gordon J. Berman. Optogenetic dissection of descending behavioral control in Drosophila. *eLife*, Jun 2018.

[2] Wu Y Dickson BJ Bidaye SS, Machacek C. Neuronal control of Drosophila walking direction. *Science*, 344(6179):97–101, Apr 2014.

[3] Shigehiro Namiki, Michael H. Dickinson, Allan M. Wong, Wyatt Korff, and Gwyneth M. Card. The functional organization of descending sensory-motor pathways in Drosophila. *eLife*, Jun 2018.

[4] Kim SS Pulver SR Birdsey-Benson A Cho YK Morimoto TK Chuong AS Carpenter EJ Tian Z Wang J Xie Y Yan Z Zhang Y Chow BY Surek B Melkonian M Jayaraman V Constantine-Paton M Wong GK et al. Klapoetke NC, Murata Y. Independent optical excitation of distinct neural populations., 2014.

[5] Auke Jan Ijspeert, Alessandro Crespi, Dimitri Ryczko, and Jean-Marie Cabelguen. From Swimming to Walking with a Salamander Robot Driven by a Spinal Cord Model. *Science*, 315(5817):1416–1420, Mar 2007.

[6] Vivek Hari Sridhar, Dominique G. Roche, and Simon Gingins. Tracktor: Image-based automated tracking of animal movement and behaviour. *Methods Ecol. Evol.*, 10(6):815–820, Jun 2019.

[7] Alexander Mathis, Pranav Mamidanna, Kevin M. Cury, Taiga Abe, Venkatesh N. Murthy, Mackenzie Weygandt Mathis, and Matthias Bethge. DeepLabCut: markerless pose estimation of user-defined body parts with deep learning. *Nat. Neurosci.*, 21(9):1281–1289, Aug 2018.

[8] Fly Light Split-GAL4 Driver Collection, May 2020. [Online; accessed 12. May 2020].

[9] Bialek W Shaevitz JW. Berman GJ, Choi DM. Mapping the stereotyped behaviour of freely moving fruit flies. *Journal of the Royal Society Interface*, 2014.

[10] Hinton G van der Maaten L. Visualizing data using t-SNE. *Journal of Machine Learning Research*, 2008.

[11] Rajyashree Sen, Ming Wu, Kristin Branson, Alice Robie, Gerald M. Rubin, and Barry J. Dickson. Moonwalker Descending Neurons Mediate Visually Evoked Retreat in Drosophila. *Curr. Biol.*, 27(5):766–771, Mar 2017.

[12] Chin-Lin Chen, Laura Hermans, Meera C. Viswanathan, Denis Fortun, Florian Aymanns, Michael Unser, Anthony Cammarato, Michael H. Dickinson, and Pavan Ramdya. Imaging neural activity in the ventral nerve cord of behaving adult Drosophila. *Nat. Commun.*, 9(4390):1–10, Oct 2018.

[13] Damon A. Clark Brian D. DeAngelis, Jacob A. Zavatone-Veth. The manifold structure of limb coordination in walking Drosophila. *eLife*, Jun 2019.

[14] Leland McInnes, John Healy, and James Melville. UMAP: Uniform Manifold Approximation and Projection for Dimension Reduction. *arXiv*, Feb 2018.

[15] Kevin Connolly. The social facilitation of preening behaviour in Drosophila melanogaster. *Animal Behaviour*, 16(2):385–391, Apr 1968.

Appendix

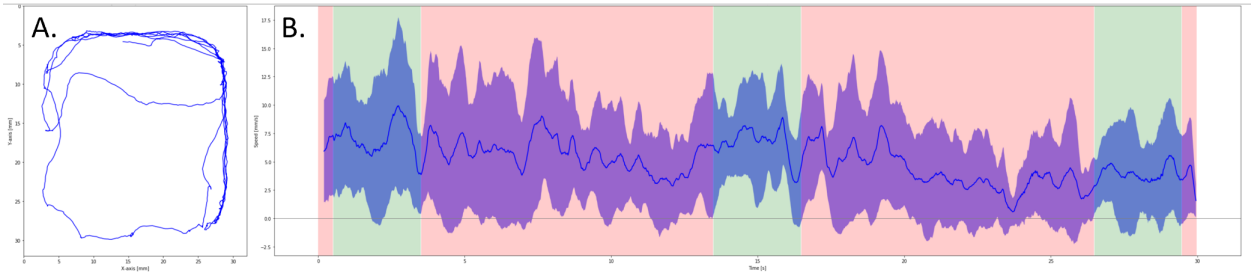

Figure 4: Kinematic results for negative control PR strain. (**A**) Position of the fly for one replica. (**B**) Averaged velocity over the strain for the full experiment. Green parts: ON periods, Red parts: OFF periods. A moving average of 30 frames was used.

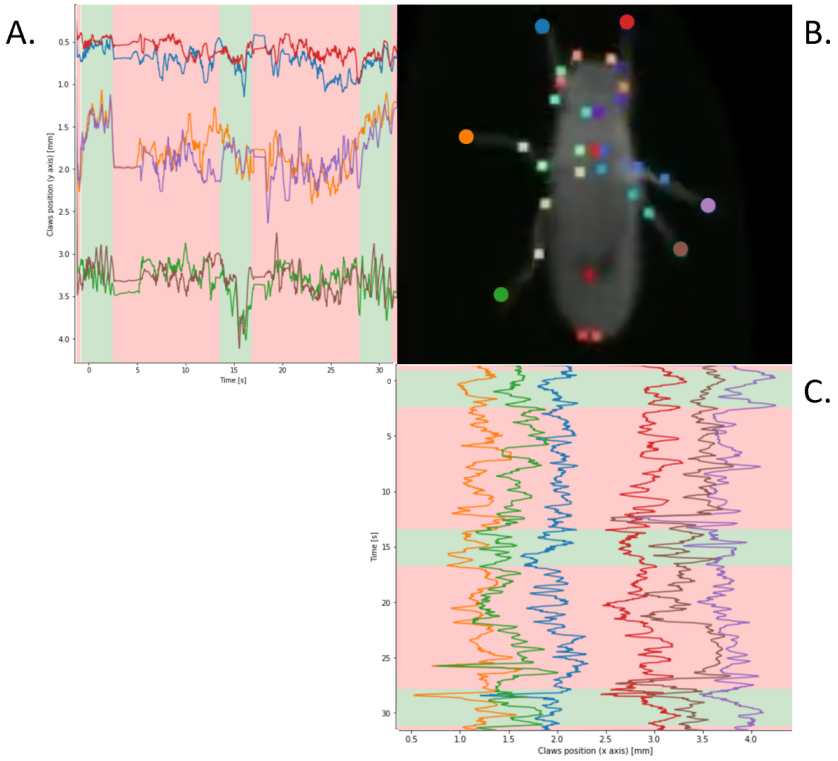

Figure 5: Example of legs positions through time over the (**A**) y-axis and (**B**) x-axis. Blue: LF, Orange: LM, Green: LH, Blue: RF, Purple: RM, Brown: RH.

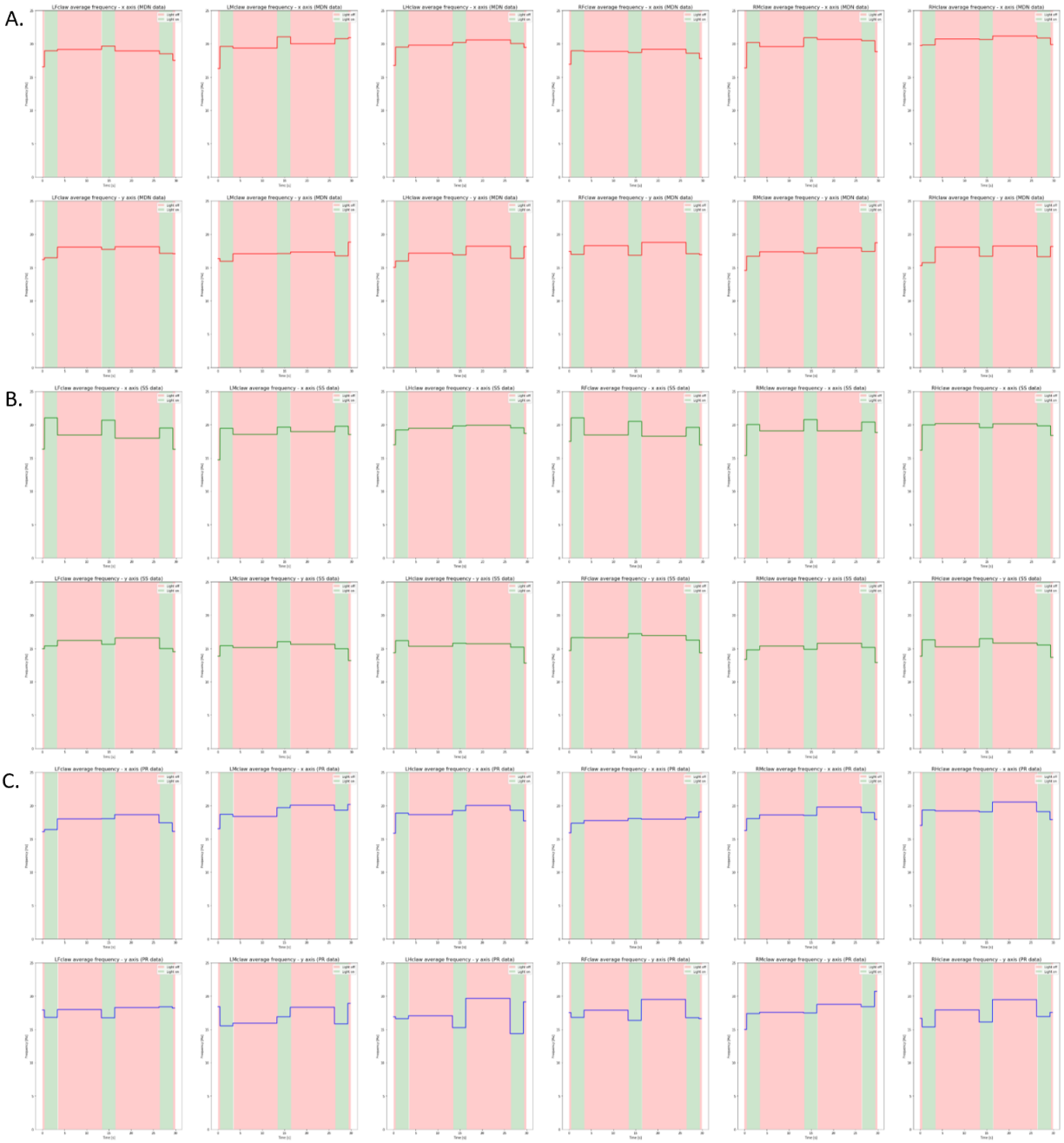

Figure 6: (**A**-**C**) Average frequency of the claws on the x-axis (top) and y-axis (bottom) over the strain. On the graphs, the y axis represents the average frequency in Hz and the x-axis is the time in seconds. From left to right: LF, LM, LH, RF, RM, RH (L: left, R: right, F: fore leg, M: middle leg, H: hind leg). A moving average of 30 frames was used. (**A**) MDN strain. (**B**) SS01540 strain. (**C**) PR strain.